

# UPCommons

Portal del coneixement obert de la UPC

<http://upcommons.upc.edu/e-prints>

---

URL d'aquest document a UPCommons E-prints:

<http://upcommons.upc.edu/handle/2117/101646>

DOI: [10.1109/WIO.2016.7745592](https://doi.org/10.1109/WIO.2016.7745592)

---

---

© 2016 IEEE. Personal use of this material is permitted. Permission from IEEE must be obtained for all other uses, in any current or future media, including reprinting/republishing this material for advertising or promotional purposes, creating new collective works, for resale or redistribution to servers or lists, or reuse of any copyrighted component of this work in other works.”

---

# First-order and multi-order diffractive lens using a device with $8\pi$ phase modulation range

Elisabet Pérez-Cabré and María S. Millán  
 GOAPI, Department of Optics and Optometry  
 Universitat Politècnica de Catalunya - BarcelonaTech,  
 Terrassa (Barcelona)–Spain  
 E-mail: elisabet.perez@upc.edu, millan@oo.upc.edu

**Abstract**— First-order and multi-order diffractive lenses are implemented using a LCoS modulator with  $8\pi$ -phase modulation range for a 514nm operation wavelength. Their performance is compared in terms of energy efficiency in the first and zero order diffractive planes. The influence of the display calibration is evaluated for each phase modulation range.

**Keywords**—diffractive optical element; spatial light modulator; multiorder diffractive lens; diffractive intraocular lens

## I. INTRODUCTION

A diffractive lens may be used as a single lightweight planar optical component or combined with others –either refractive or diffractive- to optimize the performance of an optical system. It tends to exhibit, however, severe chromatic aberrations. A diffractive lens consists of circular phase zones that introduce a radially variable phase delay in the incident wavefront (Fig.1) according to the expression  $l(r) = \exp\left\{j\left(\frac{\pi r^2}{\lambda f}\right)\right\}$ , where  $r$  is the radius,  $\lambda$  the wavelength and  $f$  the focal length. The zone spacing determines the focusing power and the surface profile of the zones have an effect on the efficiency, modulation transfer function, and chromatism. Traditionally, modulo  $2\pi$  diffractive lenses were designed to work with high efficiency in the first diffractive order, which entails phase jumps of  $2\pi$  for the design wavelength at each zone boundary [1,2]. When this phase jump is reduced to  $\pi$ , the diffractive lens produces a low efficiency image (approximately 40%) in the first diffractive order. The remaining 60% of the incident light is distributed between the zero order (about 40%) and higher orders (about 19%). If the sawtooth pattern of  $\pi$  phase echelettes is cut into the base curved surface of a refractive carrier lens, the resulting hybrid refractive-diffractive optical component is named diffractive bifocal lens because it has two focusing powers. The carrier lens power combined, on the one hand, with the zero diffractive order of the blazed lens provides the lowest power of the bifocal, and, on the other hand, with add power of the first diffracted order provides the highest power of the bifocal. This diffractive bifocal lens design has been used in intraocular lenses for providing distinct distance and near vision [3,4], thus alleviating the spectacle dependence in pseudophakic eyes. In multiorder [5] or harmonic [6] diffractive lenses, the phase jump at each zone boundary is an integer multiple  $p$  of  $2\pi$  for

the design wavelength  $\lambda_0$ , and operate in higher diffracted orders. The spectral characteristics of multiorder lenses differ from the first order case and offer potential advantages in the design of broadband and multispectral systems. The diffraction efficiency of the lens at any wavelength is  $\eta = \text{sinc}^2\left[\left(\frac{p\lambda_0}{\lambda}\right) - m\right]$ , with  $m$  the diffractive order. Those illuminating wavelengths satisfying  $\lambda = p\lambda_0/m$  make the lens diffract 100% of their energy into the  $m$ th diffracted order and with identical optical power  $P = 1/f$ .

In ophthalmic applications, diffractive intraocular lenses with more general phase jumps of  $\alpha\pi$  have been considered to improve the optical performance of the lens in various aspects: multifocality, depth of focus extension, achromatic property, apodization and distribution of the energy efficiency among the main diffractive orders (see, for instance, [7]).

Liquid crystal (LC) spatial light modulators (SLMs) have been extensively used to implement programmable diffractive lenses. Initially, these devices had a limited phase dynamic range, not even reaching  $2\pi$  and often with amplitude and phase coupled modulation. Nowadays, modern liquid crystal on silicon (LCoS) modulators provide phase-only modulation with larger phase modulation dynamic range that may reach  $4\pi$  or even  $8\pi$  for some operating wavelength. These devices are useful to test new designs of first-order, second-order [8] and higher order [9] diffractive optical elements with no need of fabricating them physically, and with the often-stated

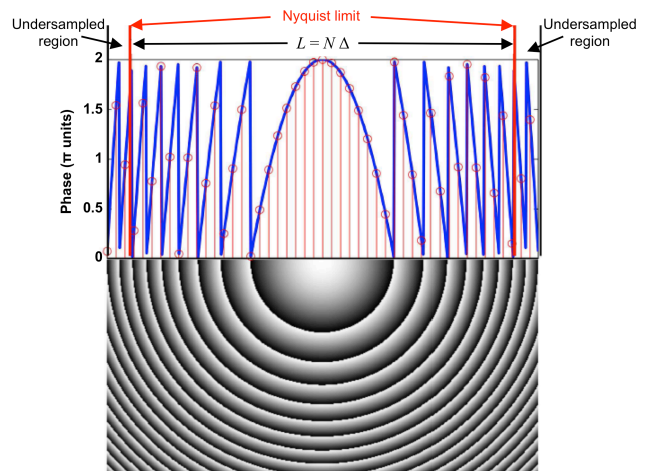


Fig. 1. Top: Plot of the phase delay function of a modulo  $2\pi$  diffractive lens. Bottom: Phase distribution encoded in grey levels.

advantages of flexibility and speed at a reasonable cost. In addition, shadowing effects produced by too high echelettes are overcome when the multiorder diffractive element is implemented by a SLM. But the initialization of such devices is not always straightforward; moreover, they must be carefully characterized to fully take advantage of their potential capabilities.

In this work, we use a LCoS modulator with a phase modulation range up to  $8\pi$  for a given operating wavelength of (514nm), previously characterized in our laboratory, to implement first- and multi order diffractive lenses with different calibration conditions. This is an initial step towards a deeper exploration of the device capabilities for designing and testing more complex diffractive bifocal and optical components. We provide experimental results and discuss on them and outline the main conclusions in the last part of the paper.

## II. EXPERIMENTAL RESULTS

### A. Device specifications and general experiment design

We have used a parallel-aligned nematic LC device of LCoS-SLM technology from (Holoeye-Pluto-BB-HR), with  $1920 \times 1080$  pixels of size  $8 \times 8 \mu\text{m}^2$  and refreshing rates of 60 Hz. The Nyquist focal length [10] is  $f_N = N\Delta^2/\lambda$ , where  $\Delta$  is the pixel pitch and  $N \times N$  the array of square pixels of the display. As a rule of thumb, the range of focal lengths must meet the condition  $f_N < f < 50f_N$  [10]. In our experimental conditions, the Nyquist focal length is 124.5mm. The operating wavelength was 514nm of a tunable Ar ion laser, with which we obtained  $8\pi$  rad phase modulation range. A half-wave plate was used to adjust the polarization of the incident beam on the modulator.

We performed two calibrations of the modulator so as to optimize its performance for either  $2\pi$  or  $8\pi$  rad with the illuminating wavelength of 514nm (Fig. 2). For a given calibration, the phase distribution encoded in 256 grey levels corresponding to a diffractive lens of 250mm focal length was sent to the modulator display via PC. The diffraction patterns were acquired with a CCD camera (PCO.1600, with 1600x1200 pixel resolution, 14 bit dynamic range).

### B. Results

In the first experiment we used the calibration optimized for a linear response of the device to modulo  $2\pi$ , that is, to

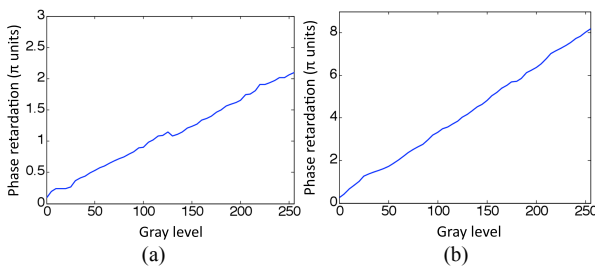


Fig. 2. Experimental calibration curves for (a)  $2\pi$  and (b)  $8\pi$  phase modulation.

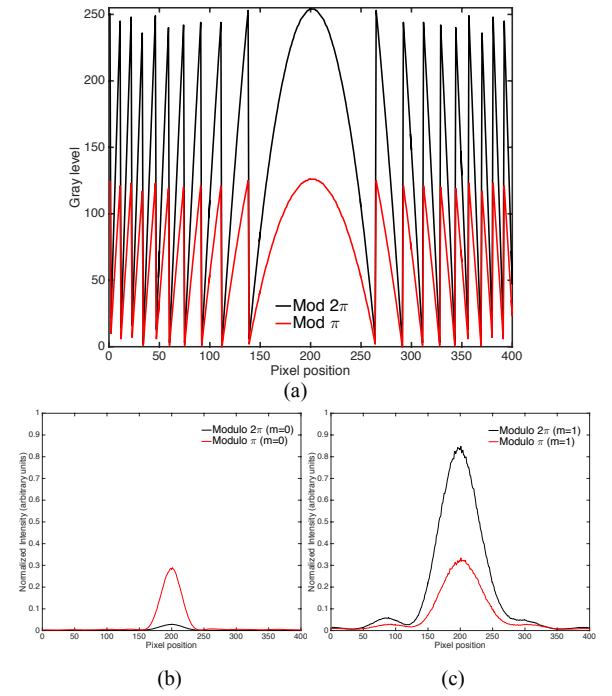


Fig. 3. a) Plots of the phase function of diffractive lens with modulo  $2\pi$  (black line) and  $\pi$  (red line). b) Intensity profile of the diffracted pattern in the zero order (brought to focus with an auxiliary lens of 20D), and c) in the first order.

linearly map 256 graylevels into the phase range of 0- $2\pi$  values. Two diffractive lenses of the same power were displayed: one, with phase jumps of  $2\pi$  at each zone boundary and, second, with phase jumps of  $\pi$  (Fig. 3a). The experimental intensity distributions diffracted in the zero and first orders are plotted in Fig. 3b and 3c, respectively. The intensity of the zero order of the  $\pi$  phase wrapping diffractive lens was measured bringing it to focus with an auxiliary lens of 20 diopters. Fig. 3b proves that a modulo  $2\pi$  lens diffracts almost all the energy in the first order, with very little energy in the zero-order; Fig. 3c shows a more balanced energy distribution between the zero and first orders (40% energy efficiency each), in good agreement with theoretical predictions.

In the second experiment, a modulo  $2\pi$  diffractive lens encoded with the calibration of the device optimized for this phase modulation range (Fig. 2a) is compared with a similar lens but encoded in modulo  $8\pi$  using the calibration optimized for such a larger phase modulation range (Fig. 2b). Figure 4 shows the phase distribution profiles of the lenses and the experimental intensities of the most efficient orders of these lenses, that is, the first order of the modulo  $2\pi$  lens and the fourth order of the modulo  $8\pi$  lens. There is a slight difference between them possibly due to the different mapping of each phase range by the 256 grey levels (finely tuned in case of the modulo  $2\pi$  lens but coarser in the case of the  $8\pi$  lens).

In the third experiment, we display the former lenses but using the same calibration of the device, that is, the one optimized for  $8\pi$  phase modulation range (Fig. 2b). Figure 5 shows the experimental results with analogous content distribution as in Fig. 4. This case shows a peak for the modulo  $2\pi$  diffractive lens somewhat less intense than the peak for the

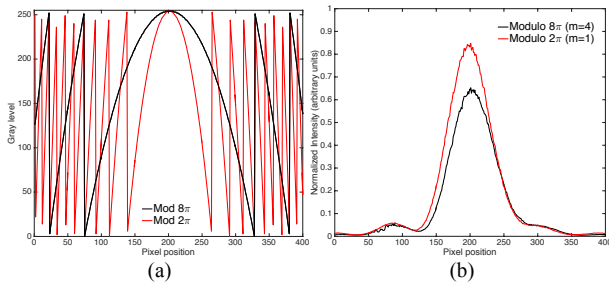


Fig. 4. Plots of the phase function of diffractive lens with modulo  $8\pi$  (black line) and  $2\pi$  (red line). b) Intensity profiles of the diffracted pattern in the first order.

modulo  $8\pi$  lens. Notice that now, the modulo  $2\pi$  lens has only a fourth part of the whole 256 gray levels to map the phase lens profile (Fig. 5a). Finally, we have repeated the last experiment, but changing the modulo  $2\pi$  diffractive lens by a  $\pi$ -diffractive lens (Fig. 6a) with the calibration optimized for  $8\pi$  phase modulation range (Fig. 2b). In Fig. 6b, the intensities of the zero order (brought to focus with an auxiliary lens) are plotted. In Fig. 6c, the experimental intensity of the fourth order diffracted pattern of the modulo  $8\pi$  lens appears with the first order diffracted pattern of the modulo  $\pi$  lens. In this case, the energy efficiency of the modulo  $\pi$  lens is no longer similar in the first and the zero orders, but twice as much.

### III. CONCLUSIONS

First-order and multi-order diffractive lenses have been implemented using a LCoS modulator with  $8\pi$ -phase modulation range for the operating wavelength of 514nm. The experimental results obtained for modulo  $\pi$ ,  $2\pi$  and  $8\pi$  diffractive lenses are in good agreement with those predicted by theory. The use of a display calibration optimized to a given phase modulation range has an influence on the energy efficiency reached in the diffracted orders.

### REFERENCES

[1] K. Miyamoto, "The phase Fresnel lens," J. Opt. Soc. Am. 51, pp.17–20, 1961.  
 [2] D. Faklis and G. M. Morris, "Optical design with diffractive lenses," Photon. Spectra. 25(11), pp. 205–208, 1991.

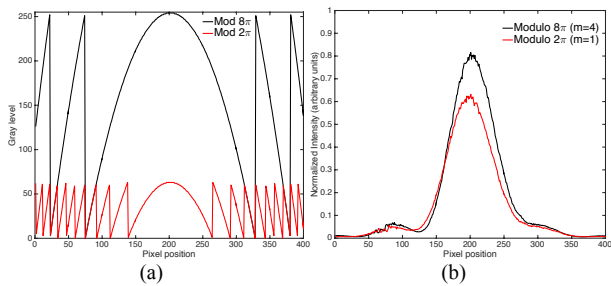


Fig. 5. Plots of the phase function of diffractive lens with modulo  $8\pi$  (black line) and  $2\pi$  (red line). b) Intensity profiles of the diffracted pattern in the first order.

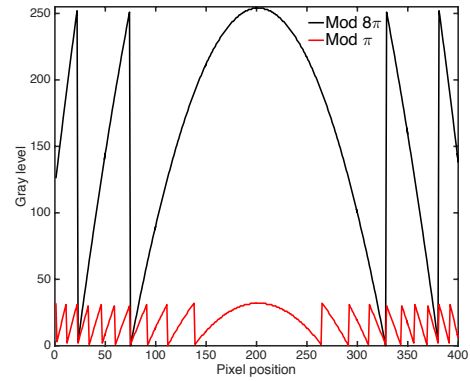


Fig. 6. a) Plots of the phase function of diffractive lens with modulo  $8\pi$  (black line) and  $\pi$  (red line). b) Intensity profile of the diffracted pattern in the zero order (brought to focus with an auxiliary lens of 20D), and c) in the first order.

[3] A.L. Cohen, "diffractive bifocal lens design", Optom. Vis. Sci. 6, pp. 461-468, 1993.  
 [4] S. Ravikumar, Bradley, A., & Thibos, L. N. "Chromatic aberration and polychromatic image quality with diffractive multifocal intraocular lenses" Journal of Cataract & Refractive Surgery, 40(7), 1192-1204, 2014.  
 [5] D. Faklis and G. M. Morris, "Spectral properties of multiorder diffractive lenses," Appl. Opt. 34(14), pp. 2462–2468, 1995.  
 [6] D.W. Sweeney and G.E. Sommargren, "Harmonic diffractive lenses," Appl. Opt. 34(14), pp. 2469–2475, 1995.  
 [7] H. A. Weeber, "Multi-ring lens, systems and methods for extended depth of focus," US Patent US2014/0168602 A1 (Jun.19, 2014).  
 [8] J. Albero, P. García-Martínez, J. L. Martínez, and I. Moreno, "Second order diffractive optical elements in a spatial light modulator with large phase dynamic range," Opt. Lasers Eng. 51, 111, 2013.  
 [9] V. Calero, P. García-Martínez, J. Albero, M. M. Sánchez-López, I. Moreno, "Liquid crystal spatial light modulator with very large phase modulation operating in high harmonic orders," Opt.Lett. 38 (22), pp. 4663-4666, 2013.  
 [10] Cottrell DM, Davis JA, Hedman TR, Lilly RA., "Multiple imaging phase-encoded optical elements written as programmable spatial light modulators," Appl.Opt. 29:2505–9,1990.